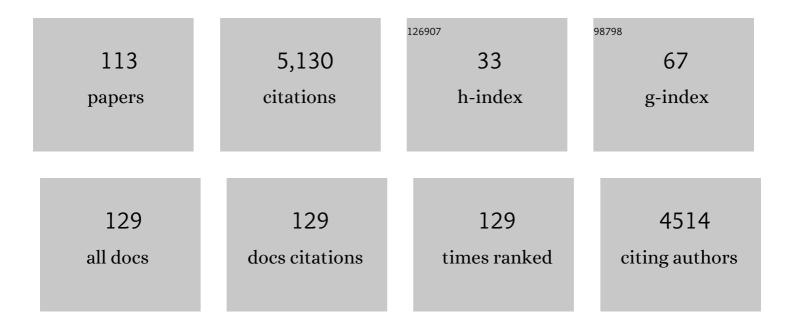
List of Publications by Year in descending order

Source: https://exaly.com/author-pdf/4763329/publications.pdf Version: 2024-02-01



#	Article	IF	CITATIONS
1	Robust Preconditioning and Error Estimates for Optimal Control of the Convection–Diffusion–Reaction Equation with Limited Observation in Isogeometric Analysis. SIAM Journal on Numerical Analysis, 2022, 60, 195-221.	2.3	1
2	Simulating epileptic seizures using the bidomain model. Scientific Reports, 2022, 12, .	3.3	2
3	Parameter-robust methods for the Biot–Stokes interfacial coupling without Lagrange multipliers. Journal of Computational Physics, 2022, 467, 111464.	3.8	4
4	Robust preconditioning for coupled Stokes–Darcy problems with the Darcy problem in primal form. Computers and Mathematics With Applications, 2021, 91, 53-66.	2.7	10
5	Modeling Excitable Tissue. Simula SpringerBriefs on Computing, 2021, , .	1.7	11
6	Parameter Robust Preconditioning by Congruence for Multiple-Network Poroelasticity. SIAM Journal of Scientific Computing, 2021, 43, B984-B1007.	2.8	6
7	Robust Preconditioners for Perturbed Saddle-Point Problems and Conservative Discretizations of Biot's Equations Utilizing Total Pressure. SIAM Journal of Scientific Computing, 2021, 43, B961-B983.	2.8	12
8	Accurate discretization of poroelasticity without Darcy stability. BIT Numerical Mathematics, 2021, 61, 941-976.	2.0	8
9	Sleep deprivation impairs molecular clearance from the human brain. Brain, 2021, 144, 863-874.	7.6	146
10	Variations in the cerebrospinal fluid dynamics of the American alligator (Alligator mississippiensis). Fluids and Barriers of the CNS, 2021, 18, 11.	5.0	14
11	Direction and magnitude of cerebrospinal fluid flow vary substantially across central nervous system diseases. Fluids and Barriers of the CNS, 2021, 18, 16.	5.0	31
12	Analysis and Approximation of Mixed-Dimensional PDEs on 3D-1D Domains Coupled with Lagrange Multipliers. SIAM Journal on Numerical Analysis, 2021, 59, 558-582.	2.3	18
13	Solving the EMI Equations using Finite Element Methods. Simula SpringerBriefs on Computing, 2021, , 56-69.	1.7	5
14	Iterative Solvers for EMI Models. Simula SpringerBriefs on Computing, 2021, , 70-86.	1.7	2
15	Improving Neural Simulations with the EMI Model. Simula SpringerBriefs on Computing, 2021, , 87-98.	1.7	2
16	Delayed clearance of cerebrospinal fluid tracer from choroid plexus in idiopathic normal pressure hydrocephalus. Journal of Cerebral Blood Flow and Metabolism, 2020, 40, 1849-1858.	4.3	43
17	Slope limiting the velocity field in a discontinuous Galerkin divergence-free two-phase flow solver. Computers and Fluids, 2020, 196, 104322.	2.5	4
18	The myodural bridge of the American alligator (<i>Alligator mississippiensis</i>) alters CSF flow. Journal of Experimental Biology, 2020, 223, .	1.7	13

#	Article	lF	CITATIONS
19	Dynamics of a neuron–glia system: the occurrence of seizures and the influence of electroconvulsive stimuli. Journal of Computational Neuroscience, 2020, 48, 229-251.	1.0	6
20	Apparent diffusion coefficient estimates based on 24 hours tracer movement support glymphatic transport in human cerebral cortex. Scientific Reports, 2020, 10, 9176.	3.3	51
21	An observation on the uniform preconditioners for the mixed Darcy problem. Numerical Methods for Partial Differential Equations, 2020, 36, 1718-1734.	3.6	5
22	Intracranial pressure elevation alters CSF clearance pathways. Fluids and Barriers of the CNS, 2020, 17, 29.	5.0	53
23	The mechanisms behind perivascular fluid flow. PLoS ONE, 2020, 15, e0244442.	2.5	43
24	Respiratory influence on cerebrospinal fluid flow – a computational study based on long-term intracranial pressure measurements. Scientific Reports, 2019, 9, 9732.	3.3	69
25	How does the presence of neural probes affect extracellular potentials?. Journal of Neural Engineering, 2019, 16, 026030.	3.5	24
26	A Mixed Finite Element Method for Nearly Incompressible Multiple-Network Poroelasticity. SIAM Journal of Scientific Computing, 2019, 41, A722-A747.	2.8	45
27	Multigrid Methods for Discrete Fractional Sobolev Spaces. SIAM Journal of Scientific Computing, 2019, 41, A948-A972.	2.8	20
28	Laplacian Preconditioning of Elliptic PDEs: Localization of the Eigenvalues of the Discretized Operator. SIAM Journal on Numerical Analysis, 2019, 57, 1369-1394.	2.3	21
29	Multi-resolution Bayesian CMB component separation through Wiener filtering with a pseudo-inverse preconditioner. Astronomy and Astrophysics, 2019, 627, A98.	5.1	18
30	Preconditioning trace coupled 3 <i>d</i> â€i <i>d</i> systems using fractional Laplacian. Numerical Methods for Partial Differential Equations, 2019, 35, 375-393.	3.6	12
31	Variational data assimilation for transient blood flow simulations: Cerebral aneurysms as an illustrative example. International Journal for Numerical Methods in Biomedical Engineering, 2019, 35, e3152.	2.1	33
32	"Bucket―cerebrospinal fluid bulk flow: when the terrain disagrees with the map. Acta Neurochirurgica, 2019, 161, 259-261.	1.7	2
33	Magnitude and direction of aqueductal cerebrospinal fluid flow: large variations in patients with intracranial aneurysms with or without a previous subarachnoid hemorrhage. Acta Neurochirurgica, 2019, 161, 247-256.	1.7	10
34	On the singular Neumann problem in linear elasticity. Numerical Linear Algebra With Applications, 2019, 26, e2212.	1.6	12
35	Introduction to Numerical Methods for Variational Problems. Texts in Computational Science and Engineering, 2019, , .	0.1	23
36	Sub-voxel Perfusion Modeling in Terms of Coupled 3d-1d Problem. Lecture Notes in Computational Science and Engineering, 2019, , 35-47.	0.3	4

#	Article	IF	CITATIONS
37	Time-Dependent Variational Forms. Texts in Computational Science and Engineering, 2019, , 233-257.	0.1	Ο
38	Variational Forms for Systems of PDEs. Texts in Computational Science and Engineering, 2019, , 259-280.	0.1	0
39	Variational Formulations with Finite Elements. Texts in Computational Science and Engineering, 2019, , 173-231.	0.1	0
40	Function Approximation by Global Functions. Texts in Computational Science and Engineering, 2019, , 7-68.	0.1	0
41	Comparison of phase-contrast MR and flow simulations for the study of CSF dynamics in the cervical spine. Neuroradiology Journal, 2018, 31, 292-298.	1.2	9
42	Brain-wide glymphatic enhancement and clearance in humans assessed with MRI. JCI Insight, 2018, 3, .	5.0	290
43	Cerebrospinal fluid volumetric net flow rate and direction in idiopathic normal pressure hydrocephalus. NeuroImage: Clinical, 2018, 20, 731-741.	2.7	73
44	Real-World Variability in the Prediction of Intracranial Aneurysm Wall Shear Stress: The 2015 International Aneurysm CFD Challenge. Cardiovascular Engineering and Technology, 2018, 9, 544-564.	1.6	78
45	Fluid dynamics in syringomyelia cavities: Effects of heart rate, CSF velocity, CSF velocity waveform and craniovertebral decompression. Neuroradiology Journal, 2018, 31, 482-489.	1.2	21
46	Parameter-Robust Discretization and Preconditioning of Biot's Consolidation Model. SIAM Journal of Scientific Computing, 2017, 39, A1-A24.	2.8	94
47	Interstitial solute transport in 3D reconstructed neuropil occurs by diffusion rather than bulk flow. Proceedings of the National Academy of Sciences of the United States of America, 2017, 114, 9894-9899.	7.1	216
48	Weakly Imposed Symmetry and Robust Preconditioners for Biot's Consolidation Model. Computational Methods in Applied Mathematics, 2017, 17, 377-396.	0.8	21
49	Numerical study of intrathecal drug delivery to a permeable spinal cord: effect of catheter position and angle. Computer Methods in Biomechanics and Biomedical Engineering, 2017, 20, 1599-1608.	1.6	9
50	Robust preconditioners for PDE-constrained optimization with limited observations. BIT Numerical Mathematics, 2017, 57, 405-431.	2.0	16
51	Direct numerical simulation of transitional hydrodynamics of the cerebrospinal fluid in Chiari I malformation: The role of cranioâ€vertebral junction. International Journal for Numerical Methods in Biomedical Engineering, 2017, 33, e02853.	2.1	18
52	A Cell-Based Framework for Numerical Modeling of Electrical Conduction in Cardiac Tissue. Frontiers in Physics, 2017, 5, .	2.1	66
53	A numerical investigation of intrathecal isobaric drug dispersion within the cervical subarachnoid space. PLoS ONE, 2017, 12, e0173680.	2.5	19
54	Robustness of common hemodynamic indicators with respect to numerical resolution in 38 middle cerebral artery aneurysms. PLoS ONE, 2017, 12, e0177566.	2.5	11

#	Article	IF	CITATIONS
55	Non-invasive assessment of pulsatile intracranial pressure with phase-contrast magnetic resonance imaging. PLoS ONE, 2017, 12, e0188896.	2.5	34
56	Computational Investigation of Cerebrospinal Fluid Dynamics in the Posterior Cranial Fossa and Cervical Subarachnoid Space in Patients with Chiari I Malformation. PLoS ONE, 2016, 11, e0162938.	2.5	16
57	Transitional hemodynamics in intracranial aneurysms — Comparative velocity investigations with high resolution lattice Boltzmann simulations, normal resolution ANSYS simulations, and MR imaging. Medical Physics, 2016, 43, 6186-6198.	3.0	30
58	Cerebrospinal fluid flow in adults. Handbook of Clinical Neurology / Edited By P J Vinken and G W Bruyn, 2016, 135, 591-601.	1.8	13
59	The association between the pulse pressure gradient at the cranio-cervical junction derived from phase-contrast magnetic resonance imaging and invasively measured pulsatile intracranial pressure in symptomatic patients with Chiari malformation type 1. Acta Neurochirurgica, 2016, 158, 2295-2304.	1.7	17
60	Preconditioners for Saddle Point Systems with Trace Constraints Coupling 2D and 1D Domains. SIAM Journal of Scientific Computing, 2016, 38, B962-B987.	2.8	24
61	Transitional flow in intracranial aneurysms – A space and time refinement study below the Kolmogorov scales using Lattice Boltzmann Method. Computers and Fluids, 2016, 127, 36-46.	2.5	22
62	Poro-elastic modeling of Syringomyelia – a systematic study of the effects of pia mater, central canal, median fissure, white and gray matter on pressure wave propagation and fluid movement within the cervical spinal cord. Computer Methods in Biomechanics and Biomedical Engineering, 2016, 19, 686-698.	1.6	32
63	Computational fluid dynamics evaluation of flow reversal treatment of giant basilar tip aneurysm. Interventional Neuroradiology, 2015, 21, 586-591.	1.1	1
64	Effect of craniovertebral decompression on CSF dynamics in Chiari malformation Type I studied with computational fluid dynamics. Journal of Neurosurgery: Spine, 2014, 21, 559-564.	1.7	15
65	A MULTI-LEVEL SOLVER FOR GAUSSIAN CONSTRAINED COSMIC MICROWAVE BACKGROUND REALIZATIONS. Astrophysical Journal, Supplement Series, 2014, 210, 24.	7.7	15
66	Spinal Fluid Biomechanics and Imaging: An Update for Neuroradiologists. American Journal of Neuroradiology, 2014, 35, 1864-1869.	2.4	37
67	Numerical simulations of the pulsating flow of cerebrospinal fluid flow in the cervical spinal canal of a Chiari patient. Journal of Biomechanics, 2014, 47, 1082-1090.	2.1	33
68	A uniformly stable Fortin operator for the Taylor–Hood element. Numerische Mathematik, 2013, 123, 537-551.	1.9	18
69	A study of wall shear stress in 12 aneurysms with respect to different viscosity models and flow conditions. Journal of Biomechanics, 2013, 46, 2802-2808.	2.1	63
70	High-resolution CFD detects high-frequency velocity fluctuations in bifurcation, but not sidewall, aneurysms. Journal of Biomechanics, 2013, 46, 402-407.	2.1	71
71	Simulating CSF Flow Dynamics in the Normal and the Chiari I Subarachnoid Space during Rest and Exertion. American Journal of Neuroradiology, 2013, 34, 41-45.	2.4	17
72	Analysis of the Minimal Residual Method Applied to Ill Posed Optimality Systems. SIAM Journal of Scientific Computing, 2013, 35, A785-A814.	2.8	9

#	Article	IF	CITATIONS
73	Estimation of CSF Flow Resistance in the Upper Cervical Spine. Neuroradiology Journal, 2013, 26, 106-110.	1.2	9
74	CSF Pressure and Velocity in Obstructions of the Subarachnoid Spaces. Neuroradiology Journal, 2013, 26, 218-226.	1.2	22
75	Effect of the Central Canal in the Spinal Cord on Fluid Movement within the Cord. Neuroradiology Journal, 2013, 26, 585-590.	1.2	8
76	Patient-Specific 3D Simulation of Cyclic CSF Flow at the Craniocervical Region. American Journal of Neuroradiology, 2012, 33, 1756-1762.	2.4	38
77	Automated Solution of Differential Equations by the Finite Element Method. Lecture Notes in Computational Science and Engineering, 2012, , .	0.3	1,283
78	On Non-Newtonian Effects in Cerebral Aneurysms: A Computational Study on 12 Patient Specific Aneurysms. , 2012, , .		0
79	A FEniCS tutorial. Lecture Notes in Computational Science and Engineering, 2012, , 1-73.	0.3	17
80	Direct numerical simulation of transitional flow in a patient-specific intracranial aneurysm. Journal of Biomechanics, 2011, 44, 2826-2832.	2.1	107
81	CSF Flow in Chiari I and Syringomyelia from the Perspective of Computational Fluid Dynamics. Neuroradiology Journal, 2011, 24, 20-23.	1.2	6
82	Preconditioning discretizations of systems of partial differential equations. Numerical Linear Algebra With Applications, 2011, 18, 1-40.	1.6	195
83	Order optimal preconditioners for fully implicit Runge-Kutta schemes applied to the bidomain equations. Numerical Methods for Partial Differential Equations, 2011, 27, 1290-1312.	3.6	3
84	Effect of Tonsillar Herniation on Cyclic CSF Flow Studied with Computational Flow Analysis. American Journal of Neuroradiology, 2011, 32, 1474-1481.	2.4	33
85	Direct Numerical Simulation of Transitional Flow in a Patient-Specific MCA Aneurysm. , 2011, , .		0
86	Flow characteristics in a canine aneurysm model: A comparison of 4D accelerated phaseâ€contrast MR measurements and computational fluid dynamics simulations. Medical Physics, 2011, 38, 6300-6312.	3.0	34
87	Construction of Preconditioners by Mapping Properties for Systems of Partial Differential Equations. , 2011, , 66-83.		0
88	Sex differences in intracranial arterial bifurcations. Gender Medicine, 2010, 7, 149-155.	1.4	47
89	Characterization of Cyclic CSF Flow in the Foramen Magnum and Upper Cervical Spinal Canal with MR Flow Imaging and Computational Fluid Dynamics. American Journal of Neuroradiology, 2010, 31, 997-1002.	2.4	51
90	Stability analysis of the inverse transmembrane potential problem in electrocardiography. Inverse Problems, 2010, 26, 105012.	2.0	13

#	Article	IF	CITATIONS
91	On the efficiency of symbolic computations combined with code generation for finite element methods. ACM Transactions on Mathematical Software, 2010, 37, 1-26.	2.9	26
92	CSF Flow Dynamics at the Craniovertebral Junction Studied with an Idealized Model of the Subarachnoid Space and Computational Flow Analysis. American Journal of Neuroradiology, 2010, 31, 185-192.	2.4	52
93	Efficient Preconditioners for Optimality Systems Arising in Connection with Inverse Problems. SIAM Journal on Control and Optimization, 2010, 48, 5143-5177.	2.1	7
94	Comparison of Aneurismal Hemodynamics Between 4-D Accelerated Phase-Contrast MR Angiography and Computational Fluid Dynamics Simulations: Initial Experience in a Canine Aneurysm Model. , 2010, , .		1
95	Can ECG Recordings and Mathematics tell the Condition of Your Heart?. , 2010, , 287-319.		0
96	Unified finite element discretizations of coupled Darcy–Stokes flow. Numerical Methods for Partial Differential Equations, 2009, 25, 311-326.	3.6	84
97	Unified framework for finite element assembly. International Journal of Computational Science and Engineering, 2009, 4, 231.	0.5	51
98	Computation of Hemodynamics in the Circle of Willis. Stroke, 2007, 38, 2500-2505.	2.0	183
99	Orderâ€Optimal Preconditioners for Implicit Runge–Kutta Schemes Applied to Parabolic PDEs. SIAM Journal of Scientific Computing, 2007, 29, 361-375.	2.8	31
100	Using Python to Solve Partial Differential Equations. Computing in Science and Engineering, 2007, 9, 48-51.	1.2	12
101	An order optimal solver for the discretized bidomain equations. Numerical Linear Algebra With Applications, 2007, 14, 83-98.	1.6	44
102	A Hybrid Approach to Efficient Finite-Element Code Development. Chapman & Hall/CRC Computational Science, 2007, , 391-420.	0.5	2
103	On the Computational Complexity of the Bidomain and the Monodomain Models of Electrophysiology. Annals of Biomedical Engineering, 2006, 34, 1088-1097.	2.5	96
104	Preconditioning of fully implicit Runge-Kutta schemes for parabolic PDEs. Modeling, Identification and Control, 2006, 27, 109-123.	1.1	21
105	Reuse of standard preconditioners for higher-order time discretizations of parabolic PDEs. Journal of Numerical Mathematics, 2006, 14, 103-122.	3.5	0
106	An observation on Korn's inequality for nonconforming finite element methods. Mathematics of Computation, 2005, 75, 1-7.	2.1	23
107	Uniform preconditioners for the time dependent Stokes problem. Numerische Mathematik, 2004, 98, 305-327.	1.9	51
108	Multigrid Block Preconditioning for a Coupled System of Partial Differential Equations Modeling the Electrical Activity in the Heart. Computer Methods in Biomechanics and Biomedical Engineering, 2002, 5, 397-409.	1.6	73

#	Article	IF	CITATIONS
109	A Robust Finite Element Method for Darcy–Stokes Flow. SIAM Journal on Numerical Analysis, 2002, 40, 1605-1631.	2.3	188
110	Numerical methods for incompressible viscous flow. Advances in Water Resources, 2002, 25, 1125-1146.	3.8	70
111	Cerebrospinal Fluid Volumetric Net Flow Rate and Direction in Idiopathic Normal Pressure Hydrocephalus. SSRN Electronic Journal, 0, , .	0.4	0
112	Physiological Background. , 0, , 1-19.		0
113	Encoderâ€decoder neural networks for predicting future FTIR spectra – application to enzymatic protein hydrolysis. Journal of Biophotonics, 0, , .	2.3	1